Bioprinting 13 (2019) e00040

Contents lists available at ScienceDirect

Bioprinting

journal homepage: www.elsevier.com/locate/bprint

# Rapid 3D bioprinting of in vitro cardiac tissue models using human embryonic stem cell-derived cardiomyocytes

Justin Liu[a], Jingjin He[b], Jingfeng Liu[b], Xuanyi Ma[c], Qu Chen[b], Natalie Lawrence[d], Wei Zhu[d], Yang Xu[b], Shaochen Chen[a,c,d,*]

[a] Materials Science and Engineering Program, University of California, San Diego, La Jolla, CA 92093, USA
[b] Division of Biological Sciences, University of California, San Diego, La Jolla, CA 92093, USA
[c] Department of Bioengineering, University of California, San Diego, La Jolla, CA 92093, USA
[d] Department of NanoEngineering, University of California, San Diego, La Jolla, CA 92093, USA

ARTICLE INFO

*Keywords:*
3D bioprinting
Cardiac tissue
in vitro model
Embryonic stem cell-derived cardiomyocytes
Calcium transients

ABSTRACT

There is a great need for physiologically relevant 3D human cardiac scaffolds for both short-term, the development of drug testing platforms to screen new drugs across different genetic backgrounds, and longer term, the replacement of damaged or non-functional cardiac tissue after injury or infarction. In this study, we have designed and printed a variety of scaffolds for in vitro diagnostics using light based Micro-Continuous Optical Printing (μCOP). Human embryonic stem cell-derived cardiomyocyte (hESC-CMs) were directly printed into gelatin hydrogel on glass to determine their viability and ability to align. The incorporation of Green Fluorescent Protein/Calmodulin/M13 Peptide (GCaMP3)-hESC-CMs allowed the ability to continuously monitor calcium transients over time. Normalized fluorescence of GCaMP3-hESC-CMs increased by 18 ± 6% and 40 ± 5% when treated with 500 nM and 1 μM of isoproterenol, respectively. Finally, GCaMP3-hESC-CMs were printed across a customizable 3D printed cantilever-based force system. Along with force tracking by visualizing the displacement of the cantilever, calcium transients could be observed in a non-destructive manner, allowing the samples to be examined over several days. Our μCOP-printed cardiac models presented here can be used as a powerful tool for drug screening and to analyze cardiac tissue maturation.

## 1. Introduction

Cardiovascular disease (CVD) is well recognized as the leading cause of death worldwide, attributing 32% of global deaths to CVD [1]. The majority of deaths are attributed to ischemic heart disease (IHD). Current treatments of IHD can only delay the progression of the disease. Thus, there is a significant need to develop new strategies to replace injured or damaged myocardium. Over the past decades, human embryonic stem cells (hESCs) have offered opportunities of repairing damaged organ such as heart [2], especially for the patients suffering loss of functional cardiomyocytes. hESCs have been extensively studied and their robust differentiation towards cardiomyocyte lineages have been well established. The strategies for generating cardiomyocytes from stem cells, maturation eliciting physiological response, and how to improve the survival of the engraftments remains a concern [3]. Potential strategies include alignment [4] and co-culture with endothelial cells and fibroblasts [5]. However, stem-cell derived cardiomyocytes are still in state of research where obtaining quality cells is both time consuming and resource intensive to differentiate with limited ability to proliferate once differentiated, a means of creating 3D micro-tissues that elicit physiological responses is necessary.

*Current work on developing 3D in vitro cardiac tissue has focused on seeding cells atop or encapsulating cells within a hydrogel-based scaffold [6,7]. While these cardiac tissue models provided support to in vitro cardiomyocyte culture, mimicking the multilayered aligned myocardium as well as the tissue mechanical property remain ultimate challenges to establishing biomimetic in vitro cardiac tissue for applications in pharmaceutical studies and screening.*

Three-dimensional (3D) printing has been more recently used to produce cell-laden 3D tissues [8,9]. Digital light-based 3D bioprinting has emerged as the next-generation of 3D printing technology, offering a superior speed, resolution, flexibility and scalability [10–12], producing millimeter-scale 3D architectures with a micron-resolution. Modified, naturally-based polymers, including gelatin [13] and hyaluronic acid (HA) [14] and synthetic PEGDA [12] can be photo-crosslinked

* Corresponding author at: Department of NanoEngineering, University of California, San Diego, La Jolla, CA 92093, USA.
*E-mail address:* chen168@eng.ucsd.edu (S. Chen).

https://doi.org/10.1016/j.bprint.2019.e00040
Received 2 October 2018; Received in revised form 20 December 2018; Accepted 3 January 2019

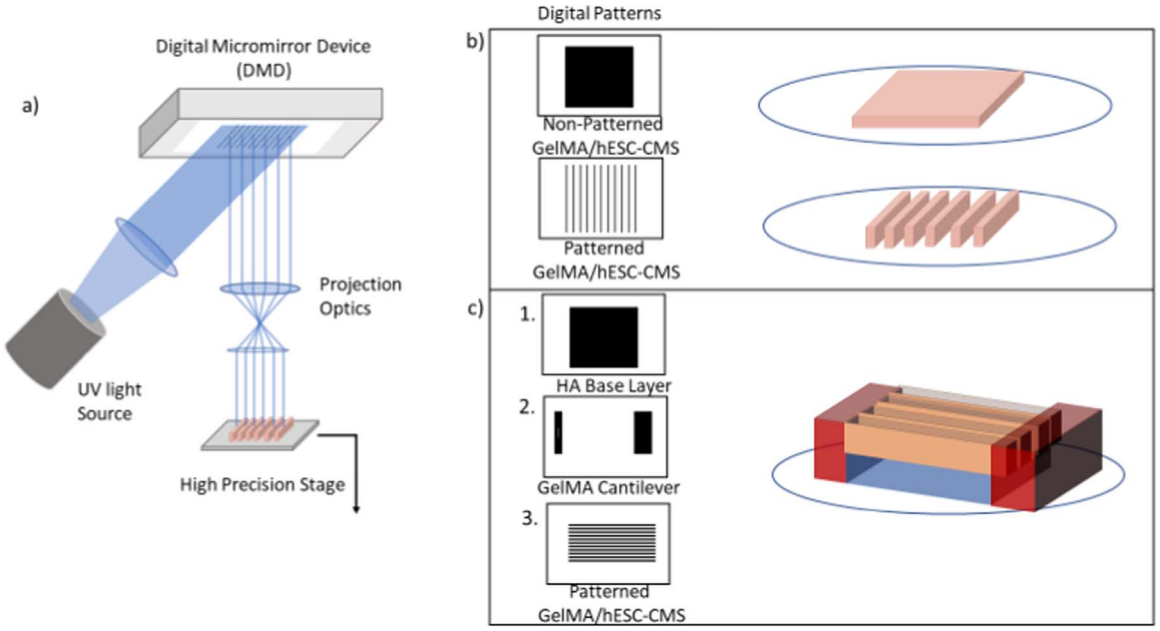


**Fig. 1.** The μCOP system and culture study parameters. a) Schematic of the μCOP system which consists of a programmable DMD, using digital masks to control millions of individual mirrors to pattern light onto a liquid volume. The computer controls the light source and exposure time and digital patterns which are paired with the high-precision stage to create 3D-scaffolds. b) Two sets of digital patterns including a simple set of parallel lines of 5% GelMA with encapsulated hESC-CMs. c) A multiprint mechanical tester including a HAGM base layer, 10% GelMA cantilevers, and parallel lines of 5% GelMA/hESC-CMs printed across the cantilevers.

using this light-based method, exposing a whole area, rather than a single point, to produce a scaffold.

In this work, we focused on the adaptation of the μCOP system (Fig. 1a) towards the direct printing of a humanized cardiac model. The μCOP system consists of a UV light source, projection optics, and a digital micromirror device (DMD), consisting of 1920 × 1080 individually controlled mirror for light projection. By sending digital patterns to the DMD and pairing patterns with a high-precision piezo-stage, patterned light can be projected onto a prepolymer solution consisting of methacrylated gelatin (GelMA) and a photoinitiator lithium 2,4,6 bisphenolphosphinate (LAP) to form a 3D construct. Furthermore, the system was optimized to encapsulate hESC-CMs within GelMA hydrogel (Fig. 1b). hESC-CMs were encapsulated in slab and line patterns to determine their viability and their ability to be patterned. Finally, we designed and directly 3D-printed a cantilever system using a 2% hyaluronic acid glycidyl methacrylate (HAGM) as a sacrificial material and 10% GelMA cantilevers for the hESC-CMs pull against (Fig. 1c). Additionally, with this structure we were able to determine the force produced by modified GCaMP3-hESC-CMs with green fluorescent protein to monitor both force and calcium transients without fluorescent dyes.

## 2. Methods

### 2.1. Differentiation of hESC-CMs cardiomyocytes

Before differentiation, hESCs were dissociated into cell aggregates by ReLeSR and seeded onto the human ES qualified Matrigel substrate coated 6-well plates. When ESCs reached 90–100% confluence, cardiomyocyte differentiation was initiated according to the protocol reported before with some modifications [15]. Briefly, hESCs were cultured in Hepes-buffered RPMI 1640 (Gibco) 2% (vol/vol) B27 minus insulin (RB-) supplemented with 12 μM CHIR99021. The following day medium was changed to HEPES-buffered (RB-) only. On day 3, the medium was changed to HEPES-buffered (RB-) supplemented with 5 μM IWP4, 2%(vol/vol). On day 5, medium was replaced with RB- media. From day 7 on, cells were maintained in HEPES-buffered RPMI 1640 supplemented with 2% (vol/vol) B27 supplement with insulin (RB+). Medium was changed every 48 h. A separate H7 cell line was created with knock-in expression of GCaMP3 following previously reported methods [16].

### 2.2. Prepolymer solution preparation

Gelatin methacrylate (GelMA) was prepared per previously described methods [10]. In brief, 10 g of gelatin (type A, bloom 300) was dissolved in 100 mL of Dulbecco's phosphate-buffered saline (DPBS) heated to 60 °C. The solution was stirred constantly and 8 mL of methacrylic anhydride was added dropwise. After three hours, the reaction was diluted with 100 mL of warm DPBS and dialyzed (14.5 kDa) against Millipore water. Water was replaced three times a day over seven days. Synthesized GelMA was frozen, lyophilized, and stored at −80°C until needed. Hyaluronic acid glycidyl methacrylate (HAGM) was prepared via modified methods [14] 1 g of HA (200 kDa) was dissolved in a 100 mL solution of 50:50 acetone: water stirring overnight. 1.8 mL of TEA was added dropwise and allowed to mix thoroughly following 1.8 mL of glycidyl methacrylate added dropwise. The solution reacted overnight and then transferred to 3500 kDa dialysis tubing and dialyzed for 48 h, replacing the water 3 times a day. Dialyzed solution was frozen and lyophilized. LAP was prepared via Michaelis-Arbuzov reaction method [17]. Prepolymer solutions prepared for these projects included 10% GelMA/0.2%LAP in DPBS, 5% GelMA/2% HA/0.2% LAP, 2% PEGDA MW 700/2% HAGM/0.2% LAP and stored at 4 °C in the dark.

### 2.3. μCOP encapsulation of hESC-CMs in hydrogel

hESC-CMs were mixed 1:1 with a 10% GelMA/0.2% LAP to a final concentration of 40 million cells per mL in 5% GelMA/0.1% LAP. The cell mixture was placed between two 250 μm spacers and a 3-(Trimethoxysilyl)propyl methacrylate (TMSPM)-treated coverslip. The sample was loaded on the μCOP printer and exposed to a digital mask for 40 s. Non-crosslinked solution was rinsed away, and the samples were placed in a 24-well plate with PSC for 10 min at 37 °C. PSC consists of 100 mM benzyloxycarbonyl-Val-Ala-Asp(O-methyl)-fluoromethyl ketone (ZVAD), 50 nM cell-permeant TAT peptide,

Bcl-XL BH4, 200 nM cyclosporine A, 100 ng/mL IGF-1, and 50 mM pinacidil with 20% fetal bovine serum (FBS) to neutralize trypsin from the cell preparation. After 24-h, samples were replaced with RPMI 1640 with 2% B27 supplement with insulin (RB+). Media was replaced every two days until fixation.

### 2.4. 3D printing of a scaffold for millimeter-scale human tissue measurements

Utilizing the μCOP system, an array of micron-scale features was built in various biopolymers using UV polymerization in a layer-by-layer fashion as previously described [11]. The main components of the fabrication system are a UV light source (Omnicure 2000), a DMD chip (Discovery 4000, Texas Instrument), and computer controlled x-y-z stages (Newport 426/433 series). A 365 nm bandpass filter with a source output of 6 W/cm$^2$ was utilized. User-defined bitmap patterns were transferred to the DMD chip and the modulated images were projected onto the photocurable pre-polymer solution through a UV- grade optical lens (Edmunds Optics). Areas illuminated by UV light crosslinked immediately, whereas dark regions remained uncrosslinked, forming the scaffold in a specific polymerization plane designated by the mask. These patterns were irradiated for 45 s at a projected UV intensity of 11 mW/cm$^2$.

*A cantilever scaffold was designed and printed using multiple materials. Initially, a 2 × 2 × 0.25 mm (l x w x h) glycydlyl methacrylate hyaluronic acid slab is exposed to light for 8 s (Fig. 1c, top), rinsed with 1X PBS and replaced with 10% GelMA. A second digital mask of one cantilever and base was exposed for 29 s (Fig. 1c, middle). The 3D printed cantilever dimensions were 1.1 × 0.25 × 0.5 mm (l x w x h). After light exposure, the 10% GelMA structure was rinsed with 1X PBS. Finally, a 2 × 1 mm scaffold, consisting of 50 μm-wide parallel lines of encapsulated hESC-CMs in 5% GelMA, was printed between the cantilever and base (Fig. 1c, bottom).* hESC-CMs were washed in PSC for 10 min at 37 °C and the PSC was replaced for culture over 24 h. Media was replaced with RB+ the following day and then every 48 h.

### 2.5. GCaMP3-hESC-CMs calcium imaging

*Samples were placed in a temperature-controlled stage under mixed air with 5% $CO_2$. GCaMP3-hESC-CMs were monitored using a Leica AF6000 inverted fluorescent microscope, imaged with 5x objective, with 348 × 260 pixel resolution (1 pixel = 7.33 μm) at a rate of around 42 frames per sec (fps). Samples were excited with 460–500 nm light and the measured fluorescence of the sample was normalized as a ratio ($\Delta F/F_0$) by taking the fluorescence level divided by the sample minima. Warm media was refreshed after imaging and samples were returned to 37°C.*

### 2.6. Immunofluorescence staining and image acquisition

All samples were fixed in 4% paraformaldehyde solution (PFA, Wako Chemicals) for 10 min at room temperature on day 3 following 3D printing. Fixed samples were then blocked and permeabilized using 2% bovine serum albumin (BSA) (Gemini Bio-Products) solution with 0.1% Triton X-100 (Promega) for 60 min at room temperature. Samples were subsequently incubated with mouse monoclonal antibodies against alpha-actinin (1:100, Abcam) overnight at 4 °C. Following three washes with PBS at room temperature, samples were incubated with fluorophore-conjugated anti-IgG antibodies (1:200, Biotium). Fluorescently stained samples were stored in PBS with 0.05% sodium azide (Alfa Aesar) at 4 °C and imaged within 1 week of staining. Confocal microscope images were acquired with a Leica SP5 microscope (Leica Microsystems).

### 2.7. Mechanical testing

To determine the force produced by the 3D-printed microtissues, acellular scaffolds were bent using a Cellscale Microsquisher. The acellular scaffolds were incubated at 37 °C 5% $CO_2$ in DPBS with 1% antibiotic 1% antimycotic. Samples were measured on day 14 and placed on their sides and submerged in a DPBS bath at room temperature. Samples were pressed using a tungsten beam, measuring the point of applied force from the base. Samples were displaced 20 μm and the sample modulus was calculated using Euler-Bernoulli beam theory [18]:

$$\omega = \frac{F}{6\Upsilon I}(3Lx^2 - x^3) \quad (1)$$

where $\omega$ is the displacement, $F$ is the force, $\gamma$ is the Young's modulus, $I$ is the 2nd moment of inertia (cuboid), $L$ is the height of the cantilever, and $x$ is the height of force application.

$$I_{cuboid} = \frac{hb^3}{12} \quad (2)$$

where $h$=length and $b$ =width of the cantilever. Forces of the aligned tissue was calculated using Eqs. (1) and (2), using the modulus of the acellular scaffolds. Videos were taken as a series of TIFF images at 10x with 2 × 2 binning at 42 frames per second. The acquired images were processed, and the displacement of the pillar was calculated using a custom MATLAB script.

## 3. Results

### 3.1. 3D direct printing of embryonic stem cell-derived cardiomyocyte in patterned hydrogel

hESC-CMs were successfully encapsulated in printed 5% GelMA slabs and line patterns (Fig. 2a). To ensure cell-cell contact of ESC-CMs within the gel, a high final cell encapsulation concentration was required, 40 million cells/mL. Scaffolds were treated with a pro-survival cocktail with 20% FBS and incubated for 10 min at 37 °C and the PSC replaced to neutralize any remaining trypsin from cell dissociation. At lower concentration i.e. 10% FBS, or without replacing the media once, the scaffolds would digest, and cells would suspend. Individual hESC-CMs were observed to beat as early as 24 h after replacing the PSC with RPMI + B27 supplement with insulin (RB+). Cells encapsulated in 5% GelMA slabs largely remained as ball-like aggregates at day 7, whereas most patterned hESC-CMs elongated along the parallel lines. *As seen in supplementary video 1, hESC-CMs printed in isotropic slabs beat synchronously, however they contract without directional preference. Whereas hESC-CMs encapsulated in the parallel lines pattern contract in the direction of patterning (supplementary video 2).* Isotropic slabs stained with calcein AM and ethidium homodimer show high viability (Fig. 2b), at 90.5 ± 0.5% viability (SEM, n = 3) at day 3. Confocal images show hESC-CMs encapsulated in 5% GelMA lines and slab express α-actinin (green, Fig. 2b). Expression of α-actinin confirmed the identity of cells as cardiomyocytes. However, a significant number of cells that expressed actin were not positive of α-actinin striations, suggesting that although they have a beating phenotype, the hESC-CMs lack a mature cardiac phenotype.

Supplementary material related to this article can be found online at doi:10.1016/j.bprint.2019.e00040.

We used hESC-CMs with a genetically encoded calcium indicator, GCaMP3 as an easier way of monitoring hESC-CMs when encapsulated in slab pattern and line patterns. Encapsulated GCaMP3-hESC-CMs required an increased exposure time of printing from 45 s to 60 s at the same cell density to produce defined structures. DIC images and

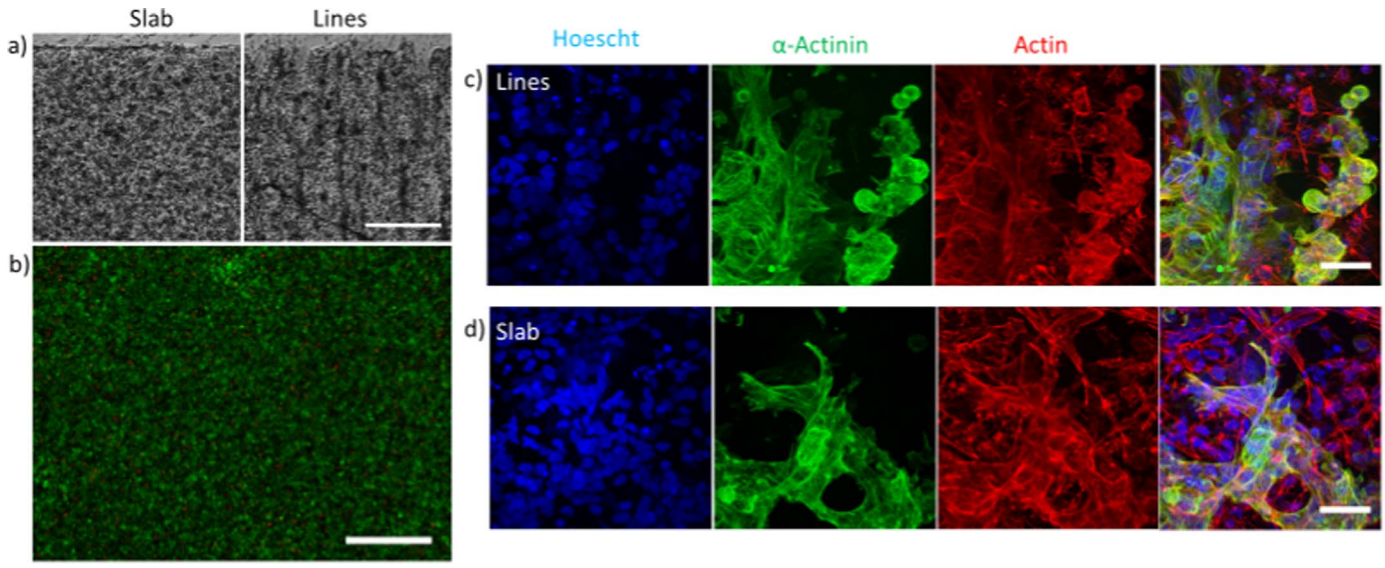


**Fig. 2.** μCOP printing of hESC-CMs in GelMA hydrogels (scale bar is 125 μm). a) DIC images of patterned hESC-CMs in slab and line patterns. b) Live/dead images of hESC-CMs (scale bar is 500 μm). Z-projections of encapsulated hESC-CMs in c) line and d) slab pattern. Samples were stained for nuclei (blue), α-actinin(green), and actin(red). Scale bar is 50 μm.

fluorescence images (in Fig. 3a) showing changes in brightness between diastole and systole are shown. Fluorescence traces (Fig. 3b) of a day 21 sample of encapsulated GCaMP3-hESC-CMs treated with ISO decreasing the average time between spontaneous beats from 2.72 ± 0.37 s (SD, n = 3) to 1.93 ± 0.057 (SD, n = 5) after treatment with 500 nM ISO and 1.96 ± 0.051 s (SD, n = 5) with 1 μM ISO. Normalized fluorescence increased by 18 ± 6% after treatment with 500 nM ISO and 40 ± 5% when treated with 1 μM ISO (SD, n = 5). Beyond normalization, no major drift or photobleaching was observed over the course of imaging, indicating stability of the system. Therefore, GCaMP3-hESC-CMs demonstrated great potential as a stable cell line for calcium transient imaging in 3D patterned scaffolds.

### *3.2. Cantilever scaffolds for 3D patterned hESC-CM tissue measurements*

Using the μCOP system, a multimaterial print consisting of 1) 2% HA/2%PEGDA base layer, 2) 10% GelMA cantilevers, and 3) a parallel line pattern comprised of 5% GelMA was produced (Fig. 4a). The final device is an elevated and patterned cardiac tissue with initial dimen-

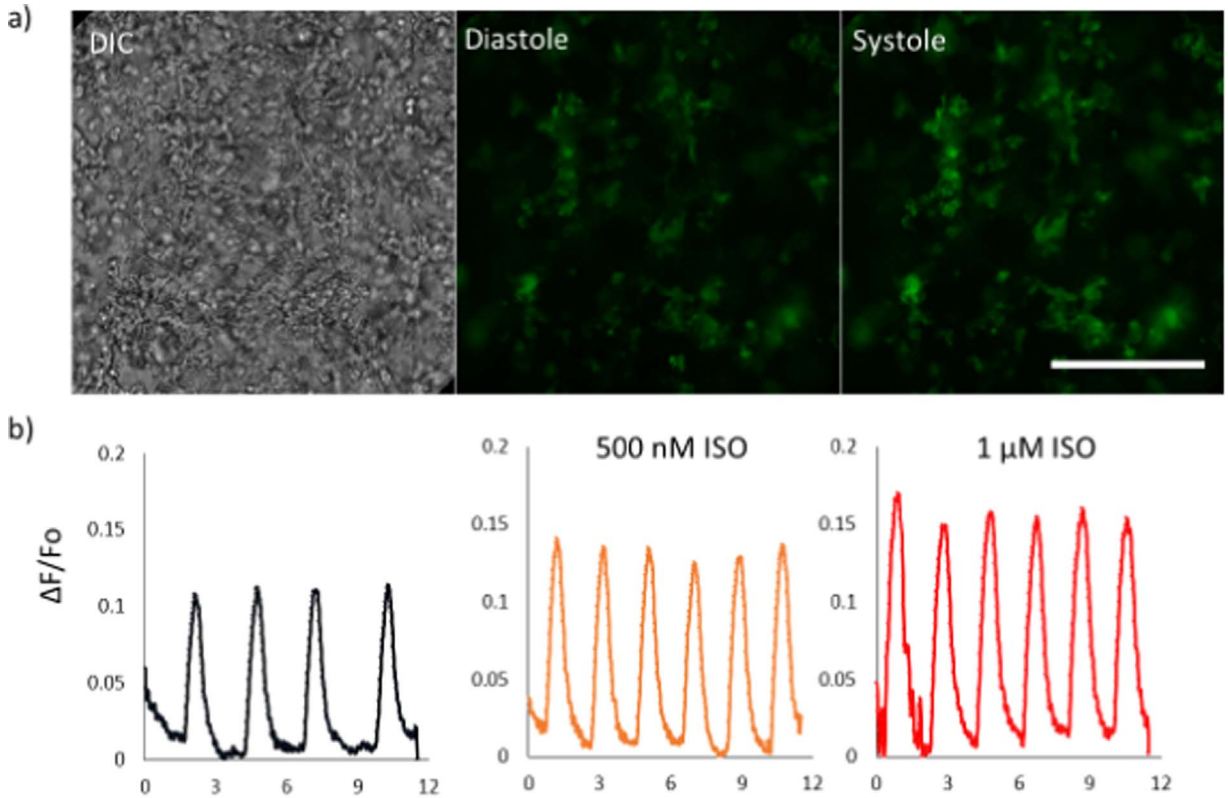


**Fig. 3.** Encapsulation of GCaMP3- modified hESC-CMs. a) A DIC and fluorescent image of GCaMP3-hESC-CMs printed in a line pattern. b) Normalized fluorescence of the scaffold after treatment with 500 nM and 1 μM ISO. Scale bar is 250 μm.

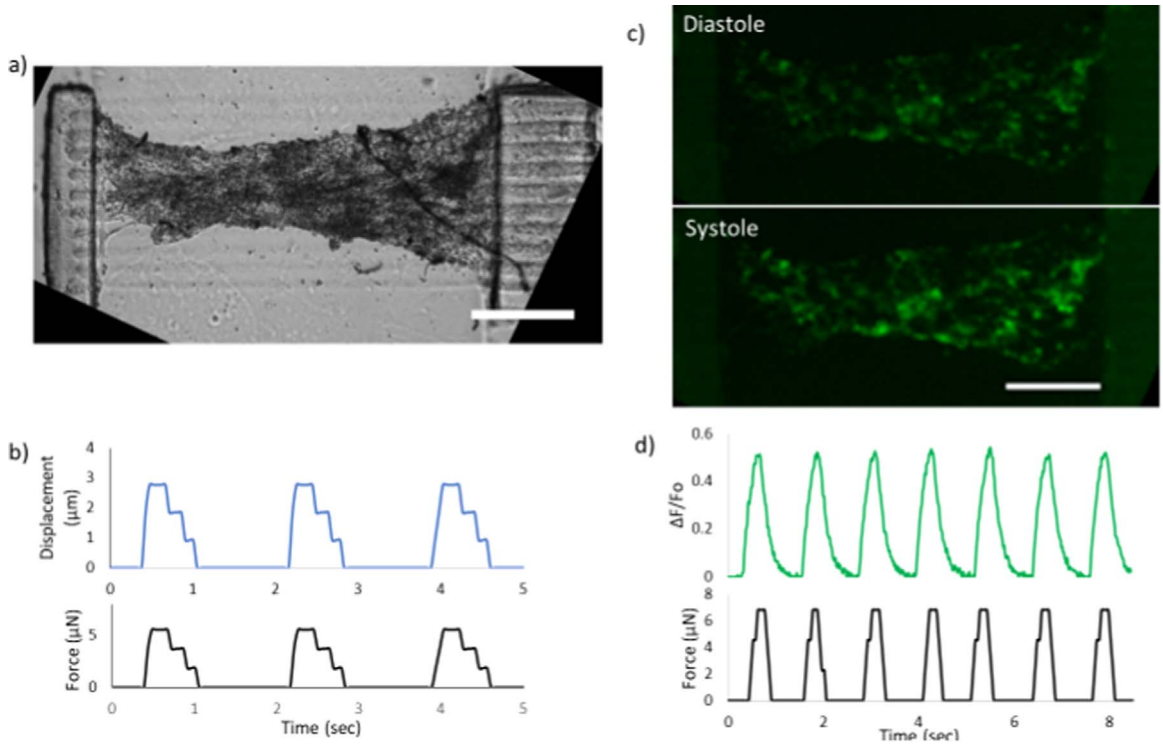


**Fig. 4.** 3D-printed force gauge to measure hESC-CMs force generation. a) Cultured hESC-CMs encapsulated in a line pattern. b) edge traces from a video recording of the pillar displacing as the tissue contracts and the calculated force. c) Fluorescent images of GCaMP-hESC-CMs printed between forces gauges during diastole (top) and systole (bottom) and d) the normalized fluorescence and force traces for the scaffold. Scale bars are 500 μm.

sions of 2 × 1 × 0.25 mm (length x width x height), and a cantilever that can be displaced with dimensions of 1.1 × 0.25 × 0.5 mm.

A sample of hESC-CMs cultured for 21 days is shown in Fig. 4b. As the 3D printed tissue tension increases, a compression of the tissue near the midline can be observed. The Young's modulus of the pillar was measured on day 14 with a cantilever-based mechanical tester (Cellscale Microsquisher), with the ability to bend the 3D printed cantilever at the midpoint where the tissue is attached to the pillar. The calculated Young's modulus of the pillar is 64 ± 6 kPa (SEM, n = 3). The ESC-CM tissue displaced the thin cantilever and a representative displacement and force trace is shown in Fig. 4b. Using the calculated Young's modulus measurement, the average force produced by 3D printed hESC-CMs across the pillar construct was 6.5 ± 0.5 μN (SEM, n = 4).

Green Fluorescent Protein/Calmodulin/M13 Peptide (GCaMP)-hESC-CMs were also printed across the cantilever system in a parallel pattern. These samples required an increase in exposure time of 60 s due to the expression of GCaMP. These samples were cultured for 21 days and spontaneous beats across the scaffold were recorded showing an increase in fluorescence between diastole and systole (Fig. 4d) with the corresponding normalized fluorescence trace show in Fig. 4e. Spontaneous beats are captured in supplementary video 3 (DIC) and supplementary video 4 (GCaMP). From edge traces, the pillar displaced up to 3.86 μm to a calculated maximum force of 6.8 μN (Fig. 4e). Thus, the designed human cardiac tissue model could be used to measure force and calcium simultaneously.

Supplementary material related to this article can be found online at doi:10.1016/j.bprint.2019.e00040.

## 4. Discussion

The ability to pattern and culture cells long term using encapsulated 3D hydrogels could be an important tool in improving maturity of hESC-CMs and hiPSC-CMs and observing disease progression. We utilized GelMA, a collagen-based photopolymerizable material, shown previously to be a favorable material for micropatterning tissue constructs and promoting cardiomyocyte attachment and spreading, [19] and LAP, a minimally toxic photoinitiator [17]. Very few groups have utilized 3D bioprinting to produce functional cardiac tissue, mainly showing the printability of cell material/cell mixtures [20,21]. Currently, hESC-CMs printed on glass coverslips still have low expression of α-actinin (Fig. 2b) although a beating phenotype was observed (supplementary video 1 and 2). The morphology of hESC-CMs were not fully extended and degradation of the scaffold was observed. Lacking cell elongation and imbalance of synthesis and degradation of the ECM proteins suggests the potential for a larger percentage of non-myocyte cells or immature cells [22,23]. *In addition to actinin and actin to show cardiac identity and cell shape, connexin-43 serves as another important marker for electrical signal transmission and therefore can be focused in future studies where mature and functional cardiac tissue is printed and studied.*

This is the first instance of GCaMP-hESC-CMs being printed in a 3D tissue setting [24,25]. The ability to detect simultaneously both calcium transients and mechanical force is especially useful for in vitro disease modeling or potentially serious side effects of drugs. For example, abnormal elevation of intracellular calcium has been reported in hiPSC-CMs derived from patients with hypertrophic cardiomyopathy with a *MYH7* mutation [26]. Enabling long-term visualization and measurement of calcium-binding and the photostability of the GCaMP sensor during acquisition compared to standard calcium-sensitive dyes like Fluo-4 and Fura-2 is promising.

Unique to μCOP system is the ability to rapidly and precisely tailor the dimensions and mechanical properties of the cantilever system and cardiac tissue by changing either digital patterns or material composition, or both [9,27]. Several groups have adapted simple cantilever systems at the mm-scale producing 7 and 55 μN of force [28,29]. Adjusting for respective tissue cross-section, the printed hESC-CM tissue twitch tension produced from this system are comparable. Furthermore, the need for cells to self-assemble may cause irregularities between samples to manifest when determining small molecule

mechanisms of action. By directly printing cardiomyocytes using the μCOP system in micron-scale structures will allow less variability between samples. Additionally, by pairing the GCaMP calcium sensor with the 3D printed cantilever system we have designed a powerful tool in determining how the calcium flux affects mechanical contractility and alternative mechanisms of disease development [25,26,30–32].

## 5. Conclusion

Being able to simultaneously assess cardiac force and calcium transient, the μCOP and aligned 3D-printed cardiac tissue demonstrate their great potential as a powerful tool in drug discovery, drug safety, and potentially tissue regeneration. Additionally, this platform promotes an improvement in cardiac function in vitro. Patient-to-patient variation in pluripotency potential and batch-to-batch variation of differentiated cells [33,34] are currently major hurdles in translating stem cell technologies for drug discovery models. Further work in maturing these tissues will be required via long-term culture and the investigation of spatial patterning of multi-cellular (e.g. cardiac fibroblast, endothelial, cardiomyocytes) tissues using the μCOP system may aid in this.

## Significance statement

In this work, we used a rapid, optical 3D printing method to directly print human stem cell derived cardiomyocytes within a patterned hydrogel. Cardiac force output was measured using a 3D printed customizable cantilever-based force system. In addition, we embedded a novel green fluorescent protein-modified hESC line sensitive to calcium as a calcium transient sensor. Using this 3D printed platform we demonstrated its potential for simultaneous recording of cardiac force and calcium transients and thus its possible use for drug screening and monitoring tissue maturation over time.

## Acknowledgements

The work was supported by a grant from the California Institute for Regenerative Medicine (RT3–07899). The UCSD Neuroscience Microscopy Shared Facility was supported by Grant P30 (NS047101).

## References

[1] G.A. Roth, M.D. Huffman, A.E. Moran, V. Feigin, G.A. Mensah, M. Naghavi, C.J.L. Murray, Global and regional patterns in cardiovascular mortality from 1990 to 2013, Circulation 132 (2015) 1667–1678.
[2] V.F.M. Segers, R.T. Lee, Stem-cell therapy for cardiac disease, Nature 451 (2008) 937–942.
[3] D.J. Mooney, H. Vandenburgh, Cell delivery mechanisms for tissue repair, Cell. Stem Cell. 2 (2008) 205–213.
[4] L. Gao, M.E. Kupfer, J.P. Jung, L. Yang, P. Zhang, Y. Da Sie, Q. Tran, V. Ajeti, B.T. Freeman, V.G. Fast, P.J. Campagnola, B.M. Ogle, J. Zhang, Myocardial tissue engineering with cells derived from human-induced pluripotent stem cells and a native-like, high-resolution, 3-dimensionally printed scaffold, Circ. Res. 120 (2017) 1318–1325.
[5] H. Sekine, T. Shimizu, K. Hobo, S. Sekiya, J. Yang, M. Yamato, H. Kurosawa, E. Kobayashi, T. Okano, Endothelial cell coculture within tissue-engineered cardiomyocyte sheets enhances neovascularization and improves cardiac function of ischemic hearts, Circulation 118 (2008) S145–S152.
[6] M.N. Hirt, A. Hansen, T. Eschenhagen, Cardiac tissue engineering: state of the art, Circ. Res. 114 (2014) 354–367.
[7] X. Ma, J. Liu, W. Zhu, M. Tang, N. Lawrence, C. Yu, M. Gou, S. Chen, 3D bioprinting of functional tissue models for personalized drug screening and in vitro disease modeling, Adv. Drug Deliv. Rev. 132 (2018) 235–251.
[8] X. Ma, X. Qu, W. Zhu, Y.-S. Li, S. Yuan, H. Zhang, J. Liu, P. Wang, C.S.E. Lai, F. Zanella, G.-S. Feng, F. Sheikh, S. Chien, S. Chen, Deterministically patterned biomimetic human iPSC-derived hepatic model via rapid 3D bioprinting, Proc. Natl. Acad. Sci. USA 113 (2016) 2206–2211.
[9] W. Zhu, X. Qu, J. Zhu, X. Ma, S. Patel, J. Liu, P. Wang, C.S.E. Lai, M. Gou, Y. Xu, K. Zhang, S. Chen, Direct 3D bioprinting of prevascularized tissue constructs with complex microarchitecture, Biomaterials 124 (2017) 106–115.
[10] P. Soman, P.H. Chung, A.P. Zhang, S. Chen, Digital microfabrication of user-defined 3D microstructures in cell-laden hydrogels, Biotechnol. Bioeng. 110 (2013) 3038–3047.
[11] J. Liu, H.H. Hwang, P. Wang, G. Whang, S. Chen, Direct 3D-printing of cell-laden constructs in microfluidic architectures, Lab Chip 16 (2016) 1430–1438.
[12] T.Q. Huang, X. Qu, J. Liu, S. Chen, 3D printing of biomimetic microstructures for cancer cell migration, Biomed. Microdevices 16 (2014) 127–132.
[13] D. Loessner, C. Meinert, E. Kaemmerer, L.C. Martine, K. Yue, P.A. Levett, T.J. Klein, F.P.W. Melchels, A. Khademhosseini, D.W. Hutmacher, Functionalization, preparation and use of cell-laden gelatin methacryloyl-based hydrogels as modular tissue culture platforms, Nat. Protoc. 11 (2016).
[14] S. Suri, L.-H. Han, W. Zhang, A. Singh, S. Chen, C.E. Schmidt, Solid freeform fabrication of designer scaffolds of hyaluronic acid for nerve tissue engineering, Biomed. Microdevices 13 (2011) 983–993.
[15] X. Lian, C. Hsiao, G. Wilson, K. Zhu, L.B. Hazeltine, S.M. Azarin, K.K. Raval, J. Zhang, T.J. Kamp, S.P. Palecek, Cozzarelli Prize Winner: robust cardiomyocyte differentiation from human pluripotent stem cells via temporal modulation of canonical Wnt signaling, Proc. Natl. Acad. Sci. USA 109 (2012) E1848–E1857.
[16] L. Borges-Pereira, B.R.K.L. Campos, C.R.S. Garcia, The GCaMP3 – a GFP-based calcium sensor for imaging calcium dynamics in the human malaria parasite Plasmodium falciparum, MethodsX 1 (2014) e151–e154.
[17] B.D. Fairbanks, M.P. Schwartz, C.N. Bowman, K.S. Anseth, Photoinitiated polymerization of PEG-diacrylate with lithium phenyl-2, 4, 6-trimethylbenzoylphosphinate: polymerization rate and cytocompatibility, Biomaterials 30 (2009) 6702–6707.
[18] E. Carrera, G. Giunta, M. Petrolo, Beam Structures, John Wiley & Sons, Ltd, Chichester, UK, 2011.
[19] H. Aubin, J.W. Nichol, C.B. Hutson, H. Bae, A.L. Sieminski, D.M. Cropek, P. Akhyari, A. Khademhosseini, Directed 3D cell alignment and elongation in microengineered hydrogels, Biomaterials 31 (2010) 6941–6951.
[20] F. Pati, J. Jang, D.-.H. Ha, S.W. Kim, J.-.W. Rhie, J.-.H. Shim, D.-.H. Kim, D.-.W. Cho, Printing three-dimensional tissue analogues with decellularized extracellular matrix bioink, Nat. Commun. 5 (1AD)1–11.
[21] R. Gaetani, P.A. Doevendans, C.H.G. Metz, J. Alblas, E. Messina, A. Giacomello, J.P.G. Sluijter, Cardiac tissue engineering using tissue printing technology and human cardiac progenitor cells, Biomaterials 33 (2012) 1782–1790.
[22] S.V. Murphy, A. Atala, 3D bioprinting of tissues and organs, Nat. Biotechnol. 32 (2014) 773–785.
[23] C. Cha, P. Soman, W. Zhu, M. Nikkhah, G. Camci-Unal, S. Chen, A. Khademhosseini, Structural reinforcement of cell-laden hydrogels with microfabricated three dimensional scaffolds, Biomater. Sci. 2 (2014) 703–709.
[24] M. Maddah, J.D. Heidmann, M.A. Mandegar, C.D. Walker, S. Bolouki, B.R. Conklin, K.E. Loewke, A non-invasive platform for functional characterization of stem-cell-derived cardiomyocytes with applications in cardiotoxicity testing, Stem Cell Rep. 4 (2015) 621–631.
[25] N. Huebsch, P. Loskill, M.A. Mandegar, N.C. Marks, A.S. Sheehan, Z. Ma, A. Mathur, T.N. Nguyen, J.C. Yoo, L.M. Judge, C.I. Spencer, A.C. Chukka, C.R. Russell, P.-L. So, B.R. Conklin, K.E. Healy, Automated video-based analysis of contractility and calcium flux in human-induced pluripotent stem cell-derived cardiomyocytes cultured over different spatial scales, Tissue Eng. Part C. Methods 21 (2015) 467–479.
[26] F. Lan, A.S. Lee, P. Liang, V. Sanchez-Freire, P.K. Nguyen, L. Wang, L. Han, M. Yen, Y. Wang, N. Sun, O.J. Abilez, S. Hu, A.D. Ebert, E.G. Navarrete, C.S. Simmons, M. Wheeler, B. Pruitt, R. Lewis, Y. Yamaguchi, E.A. Ashley, D.M. Bers, R.C. Robbins, M.T. Longaker, J.C. Wu, Abnormal calcium handling properties underlie familial hypertrophic cardiomyopathy pathology in patient-specific induced pluripotent stem cells, Cell Stem Cell 12 (2013) 101–113.
[27] P. Soman, P.H. Chung, A.P. Zhang, S. Chen, Digital microfabrication of user-defined 3D microstructures in cell-laden hydrogels, Biotechnol. Bioeng. (2013) (n/a–n/a).
[28] G. Kensah, A.R. Lara, J. Dahlmann, R. Zweigerdt, K. Schwanke, J. Hegermann, D. Skvorc, A. Gawol, A. Azizian, S. Wagner, L.S. Maier, A. Krause, G. Dräger, M. Ochs, A. Haverich, I. Gruh, U. Martin, Murine and human pluripotent stem cell-derived cardiac bodies form contractile myocardial tissue in vitro, Eur. Heart J. 34 (2013) 1134–1146.
[29] Y. Morimoto, S. Mori, F. Sakai, S. Takeuchi, Human induced pluripotent stem cell-derived fiber-shaped cardiac tissue on a chip, Lab Chip 16 (2016) 2295–2301.
[30] P. Lee, M. Klos, C. Bollensdorff, L. Hou, P. Ewart, T.J. Kamp, J. Zhang, A. Bizy, G. Guerrero-Serna, P. Kohl, J. Jalife, T.J. Herron, Simultaneous voltage and calcium mapping of genetically purified human induced pluripotent stem cell-derived cardiac myocyte monolayers, Circ. Res. 110 (2012) 1556–1563.
[31] N. Sun, M. Yazawa, J. Liu, L. Han, V. Sanchez-Freire, O.J. Abilez, E.G. Navarrete, S. Hu, L. Wang, A. Lee, A. Pavlovic, S. Lin, R. Chen, R.J. Hajjar, M.P. Snyder, R.E. Dolmetsch, M.J. Butte, E.A. Ashley, M.T. Longaker, R.C. Robbins, J.C. Wu, Patient-specific induced pluripotent stem cells as a model for familial dilated cardiomyopathy, Sci. Transl. Med. 4 (2012) 130ra47.
[32] E.R. Pfeiffer, J.R. Tangney, J.H. Omens, A.D. McCulloch, Biomechanics of cardiac electromechanical coupling and mechanoelectric feedback, J. Biomech. Eng. 136 (2014) 21007.
[33] A. Kyttälä, R. Moraghebi, C. Valensisi, J. Kettunen, C. Andrus, K.K. Pasumarthy, M. Nakanishi, K. Nishimura, M. Ohtaka, J. Weltner, B. Van Handel, O. Parkkonen, J. Sinisalo, A. Jalanko, R.D. Hawkins, N.B. Woods, T. Otonkoski, R. Trokovic, Genetic variability overrides the impact of parental cell type and determines iPSC differentiation potential, Stem Cell Rep. 6 (2016) 200–212.
[34] M. Nishizawa, K. Chonabayashi, M. Nomura, A. Tanaka, M. Nakamura, A. Inagaki, M. Nishikawa, I. Takei, A. Oishi, K. Tanabe, M. Ohnuki, H. Yokota, M. Koyanagi-Aoi, K. Okita, A. Watanabe, A. Takaori-Kondo, S. Yamanaka, Y. Yoshida, Epigenetic variation between human induced pluripotent stem cell lines is an indicator of differentiation capacity, Cell Stem Cell 19 (2016) 341–354.